Crimson Publishers
Wings to the Research

Research Article

# A Model Built on Principles and Concepts that Address Discrepancies in the Classical Flat Plate Boundary Layer Theory

**Emerson Freitas Jaguaribe***

Department of Mechanical Engineering, Federal University of Paraíba, Brazil

**ISSN: 2639-0590**

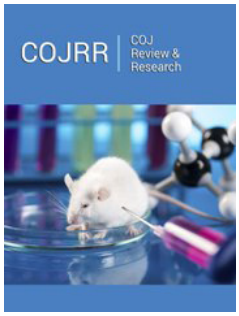


***Corresponding author:** Emerson Freitas Jaguaribe, Department of Mechanical Engineering, Brazil, emersonjaguaribe@yahoo.com.br

**Submission:** August 13, 2024
**Published:** October 03, 2024

Volume 4 - Issue 5

**How to cite this article:** Emerson Freitas Jaguaribe*. A Model Built on Principles and Concepts that Address Discrepancies in the Classical Flat Plate Boundary Layer Theory. COJ Rev & Res. 4(5). COJRR. 000598. 2024.
DOI: 10.31031/COJRR.2024.04.000598



**Abstract**

Blasius's exact solution of the boundary layer equation and von Kármán's approximate method have significantly influenced our understanding of Fluid Mechanics and related mathematical domains since the last century. However, the classical formulation of these centennial solutions is ill-suited to describe mathematically or physically the original model. Both solutions admit that the effect of a uniform flow passing over a flat plate is analogous to towing the same plate through the stationary fluid. Blasius's solution, based on a unique point on the asymptotic curve, contradicts the existence of the potential flow, and is a result of an artificial fourth boundary condition. Consequently, these classical solutions cannot precisely determine the limits of the boundary layer or predict the laminar/turbulent transition despite the typical interaction with the local Reynolds number. The main technical approaches to predict potential transition occurrence are those based on small disturbance methods or the two-equation turbulence models. Unlike classical models, the present flat plate boundary layer model enables the natural detection of regime changes without inducing flow using external forces, or relying on empirical formulations for successful closure. Comparing the proposed model results with existing classical models helps us, based on these new concepts, understand the advancements in the state-of-the-art boundary layer.

**Keywords:** General fluid mechanics; Boundary integral method; Boundary layer control; Transition to turbulence; Computational method

## Introduction

Blasius's flat plate boundary layer equation contains several critical inaccuracies in derivation and solution, Jaguaribe [1,2]. Von Kármán's flat plate integral method also exhibits similar deficiencies.

In discussing advances in boundary layer theory, Majdalani & Xuan [3] attribute pioneering work to Prandtl [4]. They credit Blasius [5] for developing the shape-preserving similarity solution and recognize Kármán [6,7] and Pohlhausen [8,9] for their contributions to the momentum-integral approach. Tertervin [10] explains that von Kármán's equation results from applying the momentum theorem to the boundary layer and refers to the results of this method as the momentum thickness and displacement thickness equations. Tertervin [10] also credits Pohlhausen [8,9] with solving the momentum equation. On the same subject, Rohsenow & Choi [11] pointed out that Blasius's solution [5] yields both velocity distribution and friction coefficient. In contrast, the alternative approximate integral method provides results only for the friction coefficient. The approximate solution is often preferred over the exact method because, in principle, it addresses both laminar and turbulent boundary layers. Pritchard & Mitchell [12] have described it as a general method. It also contributes to demonstrating the flat plate Reynolds Analogy, as noted by Welty et al. [13]. However, its formulation and application deserve some consideration, including when associated with the Reynolds analogy.

## A Comprehensive Analysis of the Two Classical Flat Plate Boundary Layer Models

### Blasius's flat plate boundary layer exact solution

Blasius [5] solved the partial differential equation

$$u\frac{\partial u}{\partial x}+v\frac{\partial u}{\partial y}=\nu\frac{\partial^2 u}{\partial y^2} \quad (1)$$

associated with the following boundary conditions

$$u=v=0 \text{ at } y=0 \quad (2)$$

$$u=U_\infty \text{ at } x=0, \text{or when } y\to\infty \quad (3)$$

and the continuity equation, in the differential form

$$\frac{\partial u}{\partial x}+\frac{\partial u}{\partial y}=0 \quad (4)$$

Where,

x and y are Cartesian coordinates;

u - the x-direction component velocity;

v - the y-direction component velocity;

$\nu$ - the fluid kinematic viscosity;

The first step to solve this mathematical problem is to convert the partial differential Equation (1) into an Ordinary Differential Equation (ODE) using a stream function $\psi$, expressed as follows:

$$\Psi=\sqrt{U_\infty \nu x}\,f(\eta) \quad (5)$$

Where

$$\eta(x)=\frac{y}{x}\mathrm{Re}_x^{\frac{1}{2}} \quad (6)$$

After conversion, Equations (1) to (5) permit the deduction of the x- and y-component velocities, that is,

$$u=U_\infty\frac{df}{d\eta} \quad (7)$$

$$v=\frac{1}{2}\sqrt{\frac{U_\infty \nu}{x}}\left[\eta\frac{df}{d\eta}-f(\eta)\right] \quad (8)$$

turning Equation (1) into

$$2\frac{d^3 f}{d\eta^3}+f\frac{d^2 f}{d\eta^2}=0 \quad (9)$$

where the solution, f, is given in terms of a series, such as

$$f(\eta)=\sum_{j=2}^{N} a_j\eta^j \quad (10)$$

and its derivatives, i.e.,

$$f'(\eta)=\sum_{j=2}^{N} j a_j\eta^{j-1} \quad (11)$$

$$f''(\eta)=\sum_{j=2}^{N} j(j-1)a_j\eta^{j-2} \quad (12)$$

$$f'''(\eta)=\sum_{j=2}^{N} j(j-1)(j-2)a_j\eta^{j-3} \quad (13)$$

where $N\to\infty$, $a_0=a_1=0$, and f′, f′′ and f′′′ represent respectively the first, second and third derivatives of the function f, in terms of $\eta$.

**Blasius's conventional solution based on constant factors α and $\eta_\infty$:** In discussing the flat plate boundary layer solution, Prandtl [4] mentioned that the power series solution, denoted as f, should be simple and asymptotic. However, a challenge arises when the solution is associated with a unique point in the asymptotic curve, f'. Upon analyzing Equation (6), it becomes apparent that by considering just a single element, $\eta$, to represent the entire plate, the "solution" is constrained to a unique value of $\eta_\infty$ for the whole plate. To address this issue, the term $\mathrm{Re}_x^{p(x)}$ should replace $\mathrm{Re}_x^{1/2}$ in Equation (6), avoiding the anomaly that limits the calculation to a single point in the curve. Thus, the new correlation should be:

$$\eta(x)=\frac{y}{x}\mathrm{Re}_x^{p(x)} \quad (14)$$

Where p(x) is a non-dimensional parameter.

Additionally, this centennial solution includes two controversial elements:

a) The first non-zero coefficient, $a_2$, see Equation (10), is considered a constant;

This fact results from the model's utilization of the similarity parameter given by Equation (6).

b) Existence of a fourth boundary condition

Considering that the first non-zero coefficient, $a_2$, is assumed as a constant and is not associated with any correlation defining it, an additional and spurious boundary condition, Equation (15), has been adopted to allow its determination

$$\left.\frac{\partial^2 f(\eta)}{\partial\eta^2}\right)_0=c \quad (15)$$

Treated as an abstraction with no natural correlation to define $a_2$, the solution of Equation (15), artificially connected to $a_2$, has traditionally been calculated by a trial-and-error method, where c is a guess. Nellis & Klein [14] describe this method applied to Blasius's solution, on page 531. They justify Equation (15) as essential because "the value of two state variables at $\eta=0$, and $\left.\frac{df}{d\eta}\right)_{\eta=0}$ are known but the value of the third state is not, which requires the implementation of an implicit numerical method that guesses a value for Equation (15). However, this explanation need be revised because what should be understood is that assuming a fourth boundary condition, in this case, implies contradicting a fundamental rule of Infinitesimal Calculus.

Criteria a) and b) do not help describe the physical model, do not align with the fundamental principle of calculus and lead to incorrect mathematical results and velocity profiles for the flat plate boundary layer that contradict Fluid Mechanics theory.

The identification of other flaws in the classical solutions appears from different perspectives. Prandtl [4] emphasized that the equation solution is simple and corresponds to the potential flow. However, upon examining Equation (8), it becomes clear that to satisfy this condition, $f(\eta_\infty)$ should be equal to $\eta_\infty$, which is not the case, as demonstrated in Howarth's [15] data or Sissom & Pitts' [16]. Reinforcing this fact, according to Rohsenow & Choi [11], the component v continues to increase, never descending to zero.

**The classical value of $2a_2$, or α:** The determination of α in the classical Blasius's model seems unnatural. A mathematical procedure known as a technique for reducing a Boundary Value Problem, BVP, to an Initial Value Problem, IVP, is used to evaluate this parameter. This approach was first used by Töpfer [17]. Unfortunately, this method is not efficient, in this case, because it yields a solution that is not unique, Van Dyke [18]. Further, as Na [19] pointed out, the boundary conditions at the initial point have to be homogeneous for this method to be applied. Klamkin [20], also citing Na [19], comments that this condition is not always necessary, adding that for considering all BVPs and IVPs, the existence and uniqueness of the latter should be tacitly assumed, which in turn will have implications for the former. In general, though, this is not true, as explained by Zeldovich & Myshkis [21], pp. 32 and 33, or Nickel [22], who affirms that the boundary conditions (u = v = 0 on y = 0, and $u \to U_\infty$ as $y \to \infty$) ensure the existence of a solution, but do not guarantee its uniqueness. These contradictions lead some authors to believe that "No known analytical solutions exist and therefore the mean profile must be determined numerically" [23] or that "The non-linear mathematical model of the problem prohibits the use of the analytical methods" [24].

## The Von Kármán's approximate solution

In 1921, von Kármán introduced the approximate integral method for the boundary layer [6,7]. In the same journal and in the NACA Technical Memorandum, a paper by Pohlhausen [8,9] appeared as a follow-up to von Kármán's work. The paper focuses on the fundamental concepts of Prandtl's boundary layer theory, delving into the mathematical formulation of the boundary layer theory, its momentum theorem and the characteristics of both laminar and turbulent boundary layers.

In reference to Pohlhausen [8,9] work on the momentum theorem, von Kármán [6,7] expressed that "The subsequent report by Pohlhausen [8,9] contains calculations for a number of practically important cases, so there is no need to delve further into this method. His calculations demonstrate that the approximate method yields results suitable for all practical purposes in cases computed by Prandtl's partial differential equations.".

In the approximate method, the continuity equation appears in differential form, see Equation (4), and u takes on the well-known binomial form

$$\frac{u}{U_\infty} = \frac{3}{2}\frac{y}{\delta} - \frac{1}{2}\left(\frac{y}{\delta}\right)^3 \qquad (16)$$

where the y-direction velocity component $v / U_\infty$ comes from Equations (4) and (16), yielding

$$\frac{v}{U_\infty} Re_x^{\frac{1}{2}} = \frac{3\sqrt{910}}{627200}\eta^2.(560 - 13.\eta^2) \qquad (17)$$

where $\eta$ represents the similarity parameter as defined by Blasius-refer to Equation (6). Figure 1 shows a plot of Equation (17) for three values of $Re_x$, 10,000, 100,000, and 500,000, and it allows the identification of two points where $v / U_\infty = 0$. These points occur at $\eta = 0$ and $\eta > 6.562$. Furthermore, Figure 1 indicates that for s, the velocity v is negative, which is somewhat unrealistic. Another limitation of this approach, similar to Blasius's [5], is the consideration of a unique $\eta_\infty$ for the entire plate.

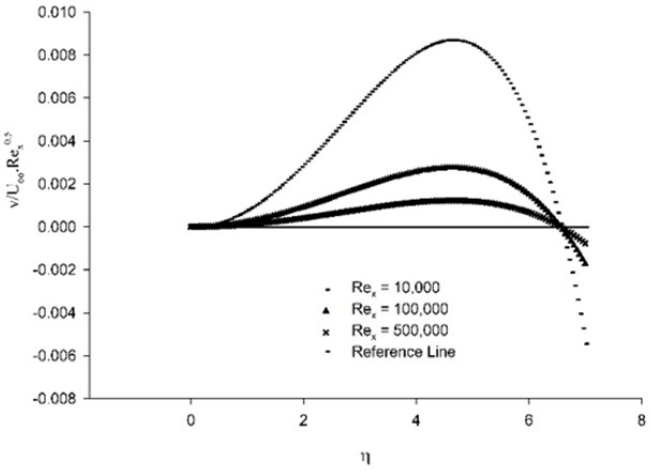


**Figure 1:** Distributions of v/U∞ in function o η for three values of Reynolds number. A reference line shows values of v=0.

Equation (17) allows the determination of the maximum value of $\eta_\infty$, 4.641, which corresponds to the classical value of $\eta_\infty$ in the von Kármán's approximate integral method. This result indicates that while Blasius determined the value of $\eta_\infty$ based on the definition of the boundary layer thickness using $0.99U_\infty$, von Kármán [6,7] chose what he believed to be the maximum value for $\eta$. It is likely that in Blasius's solution, there is only one value of $\eta_\infty$ for the entire plate. Although Von Kármán's approximation [6,7] is crucial for solving the momentum integral equation, it is flawed because as in Blasius's, this solution concerns just one point on the entire plate, and it uses a towed plate to simulate the steady uniform flow past a flat plate without accounting for the dynamic formation of the flat plate boundary layer subjected to the free stream velocity. When dealing with fluids, the Eulerian frame of reference is necessary to analyze how the properties of a moving fluid change in a specific location over time. Control volumes encompass specific locations, highlighting that the state of a flow upon entering a control surface affects the particle properties anywhere within the boundary layer and distant from the leading edge.

As seen, many inconsistencies in Blasius's flat plate problem and solution coexisted in the approximate solution. By reviewing some of Blasius's equations and re-examining the solution process, it is possible to address all these challenges. This task involves considering Equation (14), which helps define parameters like α and $\eta_\infty$ as functions of x. At the same time, it requires moving away from the concept of a towed plate and formalizing the use of a uniform flow over a flat plate. Making use of the free stream velocity will require the continuity equation in integral form, using a well-defined control volume that allows the use of Euler's reference. The quest is for a new method that can prevent some of the formal errors, enabling as well the registration of flow transitions.

## The New Flat Plate Boundary Layer Equations

### The fundamental ordinary differential equation

In the system of equations previously solved by Blasius, specifically Equations (1) to (3), the first step to solve those Equations is to convert the partial differential Equation (1) into an Ordinary Differential Equation (ODE). Instead, taking a different step, we avoid expressing the similarity parameter regarding Re raised to a constant power. To carry out this process, we define $\eta = \eta(x, y)$, such as

$$\eta(x, y) = yx^{-p}A \quad (18)$$

Where $p = p(x, U_\infty)$ is a non-dimensional variable, $U_\infty$ being the free stream velocity. If A is chosen as

$$A(\nu, U_\infty) = \left(\frac{U_\infty}{\nu}\right)^q \quad (19)$$

and $q = q(x, U_\infty)$, Equation (18) turns into

$$\eta(x, y, Re_x) = \frac{y}{x} x^{-p-q+1} Re_x^{\,q} \quad (20)$$

Where $Re_x$, the Reynolds local number is defined as

$$Re_x = \frac{U_\infty x}{\nu}$$

Then, by dimensional analysis:

$$p + q = 1 \quad (21)$$

and,

$$\eta(x, y, Re_x) = \frac{y}{x} Re_x^{\,q} \quad (22)$$

thus

$$\frac{\delta(x)}{x} = \eta_\infty(x) Re_x^{\,p-1} \quad (23)$$

where $\eta \to \eta_\infty$ when $y \to \infty$, i.e., $y \to \delta$.

On the other hand, from Equation (22):

$$\frac{\eta}{y} = \frac{Re_x^{\,q}}{x} \quad (24)$$

Figure 2 presents a sketch of a part of the boundary layer that emphasizes the x-direction velocities and the thickness of the boundary layer. A similar illustration in Figure 3 displays these velocities in non-dimensional form and the surface area z, obtained from integrating zη(η), the first derivative of z concerning η

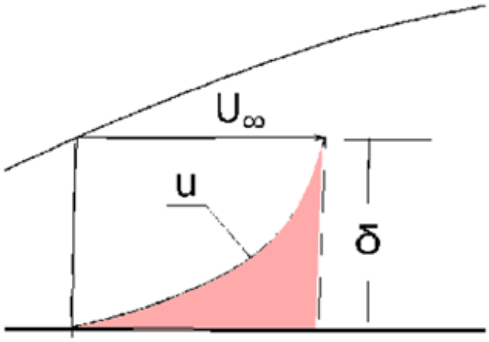


**Figure 2:** A section of the boundary layer, showing the x-direction velocities and the boundary layer thickness.

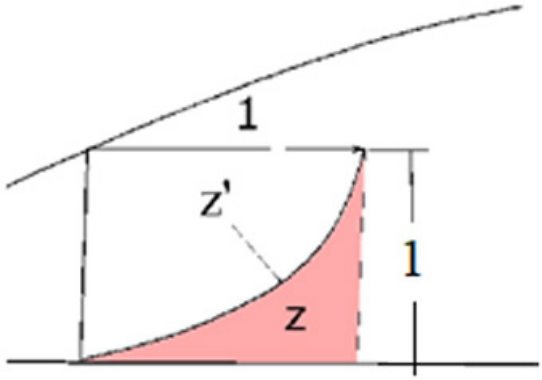


**Figure 3:** A section of the boundary layer showing the non-dimensional x-direction velocities, the area below the curve z´ and the boundary layer thickness.

Figure 3 illustrates the basis for defining the function $z(\eta)$ and displays the first derivative concerning $\eta$, given by:

$$z_\eta(\eta) = \frac{u}{U_\infty} \quad (25)$$

Consequently, from Equations (25), and (24):

$$\frac{\partial u}{\partial y} = U_\infty \frac{Re_x^{\,q}}{x} Z\eta\eta \quad (26)$$

$$\frac{\partial^2 u}{\partial y^2} = U_\infty \left(\frac{\eta}{y}\right)^2 Z\eta\eta\eta \quad (27)$$

$$\frac{\partial u}{\partial x} = -U_\infty p \frac{\eta}{x} Z\eta\eta \quad (28)$$

Where $Z\eta, Z\eta\eta, Z\eta\eta\eta$ are, respectively the shorthand notation for the first three derivatives of z in terms of η, where p > 0. From Equation (24), then:

$$dy = \frac{y}{\eta}\, d\eta \quad (29)$$

and

$$dx = -\frac{x}{\eta.p}\, d\eta \quad (30)$$

### The y-direction velocity component and the flat plate boundary layer equation

In Fluid Mechanics, a moving fluid, under progression, requires the Eulerian frame of reference, chiefly when the object of analysis is the boundary layer. Such a criterion should be applied not only during the motion disorder but also when a previously disturbed flow is recovering from the effect of the disturbance. Thus, it is necessary to choose a suitable control volume around the apparatus (the plate) to analyze the impact of the inflow on the whole boundary layer. The continuity equation should give the mass balance corresponding to the net mass that leaves and enters the control volume in a representative extension of the boundary layer, see Figure 4. Therefore, the conservation of mass computed by integral over a finite portion of the boundary layer, $\Delta x$, limited by the plate and the boundary layer outline, is the only way to calculate the due net balance, see Jaguaribe [25], resulting in Equation (31).

$$\int_0^{y'} \rho \frac{u}{U_\infty} dy.1 + \int_{x_0}^{x_1} \rho \frac{v}{U_\infty} dx.1 = \rho y'.1 \quad (31)$$

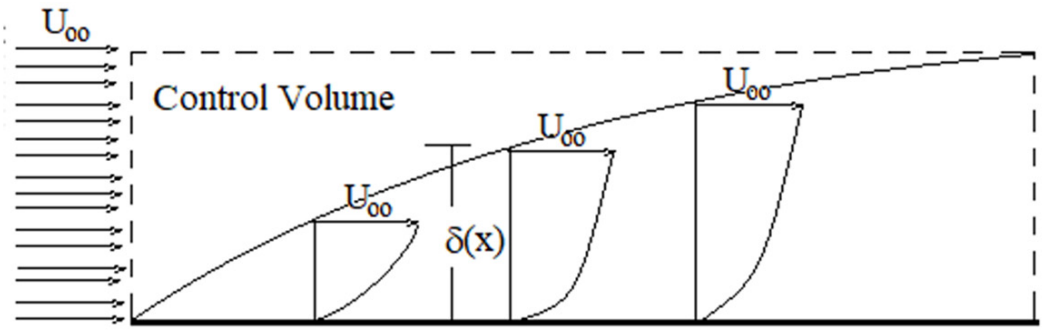


**Figure 4:** Sketch of the control volume for analysis of the classical flat plate boundary layer.

And utilizing Equations. (24), (29), (30), and Equation (25) integrated from 0 to $\delta$, after some mathematical manipulations, the new y-direction dimensionless velocity component is obtained:

$$\frac{v(x)}{U_\infty} = p(x,U_\infty)\,Re_x^{\,p(x,U_\infty)-1}\,\eta(x)(1-z_\eta) \quad (32)$$

Where $p(x,U_\infty) > 0.$

### The new flat plate boundary layer equation

Replacing Equation (1) with Equations (25) to (30) and (32), a new flat plate boundary layer equation is derived:

$$z_{\eta\eta\eta}(\eta) = \sum_{k=3}^{N} k(k-1)(k-2)a_k\eta^{k-3} \qquad (33)$$

Where,

$$\xi(x) = p(x,U_\infty)\,Re_x^{\,2p(x,U_\infty)-1} \quad (34)$$

## Solving Equation (33)

### Determining the factor $p = p(x,U_\infty)$

In considering the flow conditions induced by a towed object and in line with the similarity of velocity profiles, Schlichting [26] discusses the flat plate boundary layer on page 136 and proposes excluding the region immediately behind the leading edge. However, to represent accurately the presumed existence of a uniform flow within the physical model, it is necessary to characterize and describe all relevant mathematical aspects thoroughly. To ensure a suitable series solution for Equation (33), the x-direction velocity, u, must satisfy two distinct situations.

1) for all y ≠ 0, $\lim_{X^- \to 0} u = U_\infty$

2) for all x, $\lim_{y \to \delta} u = U_\infty$

Consequently, the only series capable of meeting these requirements is:

$$z_\eta(\eta) = \sum_{k=0}^{n} a_k\eta^k \quad (35)$$

Where,

$$a_2 = \frac{1}{(2.\eta_\infty)}. \quad (36)$$

And $a_0 = a_1 = 0$, then, from Equations (35) and (36):

$$z(\eta)_\eta = \frac{\eta}{\eta_\infty} + \sum_{k=3}^{n} k a_k \eta^{k-1} \quad (37)$$

$$z_{\eta\eta}(\eta) = \sum_{k=2}^{N} k(k-1)a_k\eta^{k-2} \quad (38)$$

$$\xi.\eta.(2Z_\eta - 1)Z_{\eta\eta} + Z_{\eta\eta\eta} = 0 \qquad (39)$$

Where $N = 2k+3.$ And given Equation (43) and the natural boundary condition

$$z_\eta(\eta_\infty) = 1 \quad (40)$$

We have

$$\sum_{k=3}^{n} k a_k \eta_\infty^{\,k-1} = 0 \quad (41)$$

Diverging from the classical Blasius's solution, the distribution of the non-dimensional x-direction velocity in terms of η given by Equation (41) forms a quite perfect straight line, as will be shown later.

The two other natural boundary conditions are:

$$z(0) = 0, \quad (42)$$

$$z_\eta(0) = 0. \quad (43)$$

Considering Equations (33), (34), and (37) - (39), and the boundary conditions given by Equations (40), (42), and (43), we come to:

$$\xi + 6a_3 + 24a_4\eta_\infty + (6\xi a_3 + 60a_5)\eta_\infty^{\,2} + (12\xi a_4 + 120a_6)\eta_\infty^{\,3} + (20\xi a_5 + 210a_7)\eta_\infty^{\,4} + \cdots = 0 \quad (44)$$

Evaluating both sides of Equation (44), we find out that

$$a_4 = a_6 = a_8 = a_{10} = a_{12} = \ldots = 0 \quad (45)$$

the odd terms being given by:

$$a_{2j+3} = (-1)^{j+1}\frac{(2^j j!)}{(2j+3)!}\xi^{j+1} \quad (46)$$

j = 0, 1, 2, ...

Thus, Equation (33) becomes

$$-\frac{1}{2} + \frac{\eta_\infty^2}{12}\xi - \frac{\eta_\infty^4}{90}\xi^2 + \frac{\eta_\infty^6}{840}\xi^3 - \frac{\eta_\infty^8}{9450}\xi^4 + \frac{\eta_\infty^{10}}{124740}\xi^5 - \ldots = 0 \quad (47)$$

That is,

$$-\frac{1}{2} + \frac{1}{12}\lambda - \frac{1}{90}\lambda^2 + \frac{1}{840}\lambda^3 - \frac{1}{9450}\lambda^4 + \frac{1}{124740}\lambda^5 - \ldots = 0 \quad (48)$$

Where,

$$\lambda = \eta_{\infty}^{2}\xi \quad (49)$$

Equation (48) is solved using the Mathcad´s Release 15 root function with four arguments and 301 terms, determining λ = 116.74438. It is clear that, in this case, only positive and Real values can be valid as a solution. In the Fundamental Theorem of Algebra, every non-constant polynomial with complex coefficients has a root in the complex numbers - Fine and Rosenberger [27], as in Descartes's rule of signs - Meserve [28]. Thus, the polynomial in Equation (48) has one and just one Real root when considering an even number of terms, allowing the determination of a valid root λ.

**The coefficient $a_2$**

We saw that one critical difficulty in Blasius's [5] solution was to set all the coefficients of his series solution in terms of the first non-null term, $a_2$, without being able to define it through a representative correlation. To overcome this misconception, we should interpret the second derivative of the series solution, see Equation (38) at $\eta = 0$, to conclude that

$$2a_2 = z_{\eta\eta}(0), \quad (50)$$

Where $2a_2$ corresponds to the tangent of the angle α(x), which intersects a common point both in the curve u and on the plate: α(x) is formed by the tangent line itself and a line perpendicular to the plate, meeting the common point. Thus,

$$2a_2(x) = \beta(x) = \tan(\alpha(x)) \quad (51)$$

Then,

$$a_2(x) = \frac{\tan(\alpha(x))}{2} \quad (52)$$

And following from Equation (36)

$$\eta_{\infty} = \frac{1}{\tan(\alpha(x))} \quad (53)$$

Where,

$$\alpha(x') < \frac{\pi}{2}. \quad (54)$$

The angle $\alpha(x')$ is a result of the viscosity effect and a linear function of x, given by:

$$\alpha(x') = \frac{\pi}{2}(1 - x') \quad (55)$$

Where,

$$x' = \frac{x}{L} \quad (56)$$

and when $L \geq x_C$, then $0 < x' \leq 1$. $x_C$ represents the critical distance limit where the transition region begins. In our calculations, $x_C$ is equal to 1m.

The present theory considers a perfectly uniform and parallel flow moving over a smooth surface without any inflection points in the velocity profiles. The flow is not affected by any receptivity process, as described by Bhoraniya et al. [29] nor influenced by any environmental forcing effects, Morkovin & Reshotko [30]. The critical Reynolds number, $Re_C$, is $5x10^5$, and the kinetic viscosity is $1.263x10^{-4}$ $m^2/s$. Consequently, at a distance of 1 meter (L=1 m), $Re_L = Re_C$, when $U_\infty$ is 63.15m/s.

Given Equation (55), under specific conditions dependent only on fluid viscosity, inequality (54) must be redefined as:

$$-\frac{\pi}{2} < \alpha(x) < \frac{\pi}{2} \quad (57)$$

In Equation (55), if x´>1, it indicates that the flow goes past the limit of the laminar zone and moves into the transition zone. This condition confirms that the local Reynolds number can be less than $5x10^5$ without preventing transition from happening.

The factor $p(U_\infty, x)$ is a significant element in the equations of this model. For its evaluation, we use Equation (49) combined with Equation (34) expressed in the logarithm form, i.e.,

$$\ln(p.\eta_{\infty}^{2}) + (2.p - 1).\ln(Re_x) - \ln(\lambda) = 0 \quad (58)$$

with the aid of the root function of Mathcad´s Release 15 with four arguments.

## Evaluation of the boundary layer thickness, $\delta(x)$

Taking p and Equations (26) and (53), $\delta(x)$ is evaluated:

$$\frac{\delta(x,U_\infty)}{x} = \eta_\infty(x) Re_x^{p(U_\infty,x)-1} \quad (26)$$

Comparing Equation (26) with the traditional Blasius's [5] expression, we realize that, in Blasius's [5] equation, 5.0 replaces $\eta_\infty(x)$, and 0.5, $p(U_\infty, x)$ which gives

$$\frac{\delta}{x} = \frac{5.0}{Re_x^{0.5}} \quad (59)$$

Figure 5 shows curves plotted from Equations (59) and (26) for four different free stream velocity magnitudes: $U_\infty$ = 35.15 m/s, 49.15 m/s, 63.15 m/s, and 70.15 m/s. The choice of $U_\infty$ =63.15 m/s ensures that at 1m from the leading edge, the Reynolds number reaches the critical value of $5x10^5$.

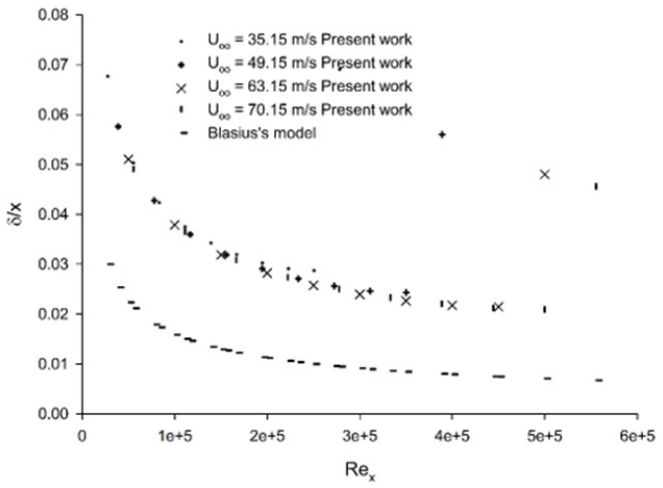


**Figure 5:** Results for the boundary layer thickness, δ/x, related to four free stream velocities, calculated using the present model and Blasius's.

Plotting Blasius's Equation (59), for various free stream velocity values mentioned earlier, results in a unique curve, as shown in Figure 5. In simple terms, in Blasius's model, variations in the Reynolds number magnitude do not indicate a different flow

regime, except for the laminar flow, regardless of the Reynolds number magnitude. It is also worth noting in Figure 5 that the curves obtained by the current model and those by Blasius's [5] have a very similar shape and are almost parallel. From a practical standpoint, the flow over a flat plate begins in the laminar regime but transitions to the transient regime. The Blasius model is unable to simulate ongoing flows and requires improvement.

In contrast, the current model is responsive to changes in the free stream velocity and the Reynolds number, automatically adjusting the magnitude of the p-value in response. This flexibility results in a specific alteration in the boundary layer outline, noticeable from a specific location on the plate, associated with the critical Reynolds number. From this point onwards, the boundary layer thickness begins to increase, leading to a significant growth in its length, ultimately causing instability in the boundary layer.

## Non-dimensional velocity components

### The non-dimensional x-direction velocity $u/U_\infty$

Using Equations (37) and (41) the non-dimensional x-direction velocity, $u/U_\infty$, component's correlation, becomes:

$$\frac{u}{U_\infty} = \frac{\eta}{\eta_\infty} \quad (60)$$

Figure 6 illustrates distributions of the non-dimensional x-direction, $u/U_\infty$, in terms of η along a plate. The local Reynolds number, $Re_x$, varies at different points due to the position and changes in the local free stream velocity, $U_\infty$. The distributions in Figure 6 correspond to four of the 301 stations used, identified by x/L values along the plate (0.0333, 0.2000, 0.3667, and 0.5333). Each is associated with three free stream velocities: 37.89m/s, 50.52m/s and 63.15m/s. In Figure 6, all velocity profiles show kinematic similarity, like Blasius's classical formulation. As noticed, the farther the distance from the leading edge, the smaller the angle formed by the $u/U_\infty$ and the x-axis.

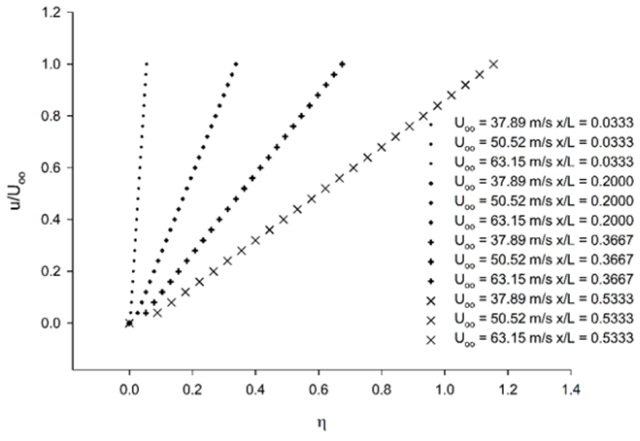


**Figure 6:** Non-dimensional x-direction velocity distributions in terms of η, related to three different positions on the flat plate and three values of the free stream velocities.

The velocity profiles shown in Figure 7 differ from the typical y-direction profiles obtained by Blasius's solution, see, for example, Rohsenow & Choi [11] or Puttkammer [31]. Unlike the typical profiles, these profiles comply with Prandtl's boundary layer concept because at the plate and the limit of the boundary layer, $v/U_\infty = 0$. Additionally, the kinematic similarity is satisfied, as shown in Figure 7. The non-dimensional velocity, $v/U_\infty$, decreases proportionally inverse to the free stream velocity magnitude for points located on the same position related to the leading edge.

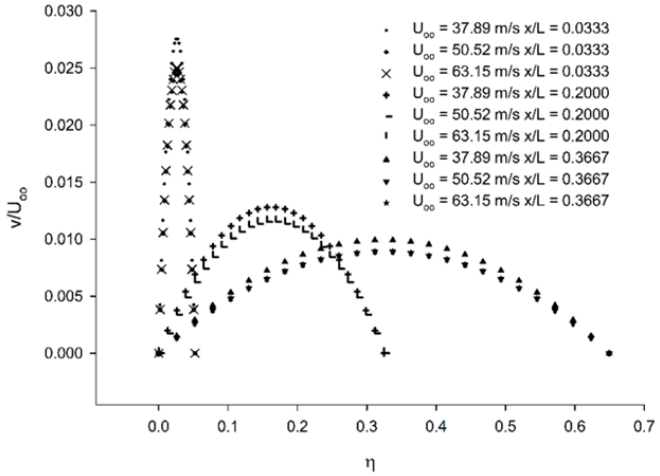


**Figure 7:** Nondimensional y-direction velocity distribution concerning several points on the plate.

## The local skin friction coefficient, $C_{f,x}$

By definition,

$$C_{f,x} = \frac{\tau w,x}{\frac{\rho U_\infty^2}{2}} = \frac{\mu \frac{\partial \mu}{\partial \mu}\Big)_{y=0}}{\frac{\rho U_\infty^2}{2}} \quad (61)$$

Then, from Equations (61) and (26)

$$C_{f,x} = \frac{2}{z_{\eta\eta}(0)} . Re_x^{-p(x,U_\infty)} \quad (62)$$

Note that considering $p(x, U_\infty) = 0.5$ and $z_{\eta\eta}(0) = 0.332$, the expression for the local skin friction coefficient related to Blasius's solution is retrieved:

Figure 8 shows the theoretical behavior of the local skin friction curves calculated by Equation (62), in the present work, and by Equation (63) from Blasius´s [5] model.

$$\frac{C_{f,x}}{2} 0.332 Re_x^{-\frac{1}{2}} \quad (63)$$

The data from Equation (63) can be seen in Figure 8 forming a consistent curve with continuously decreasing slopes. According to Clayton et al. [32], this curve represents a boundary layer starting as laminar and transitioning to a turbulent boundary layer after a certain Reynolds number. Surprisingly, the local skin coefficient values, calculated using Equation (63), continue to decrease for cases related to the transition region, specifically for $Re_x > 5x10^5$. In contrast, Equation (62) allows plotting curves that exhibit upward concavity when shifting from laminar to turbulent flow regime. The transition from laminar to turbulent on a flat plate also involves a considerable change in the resistance to flow, shown in this case as an augmentation in the skin friction value, Schlichting [26].

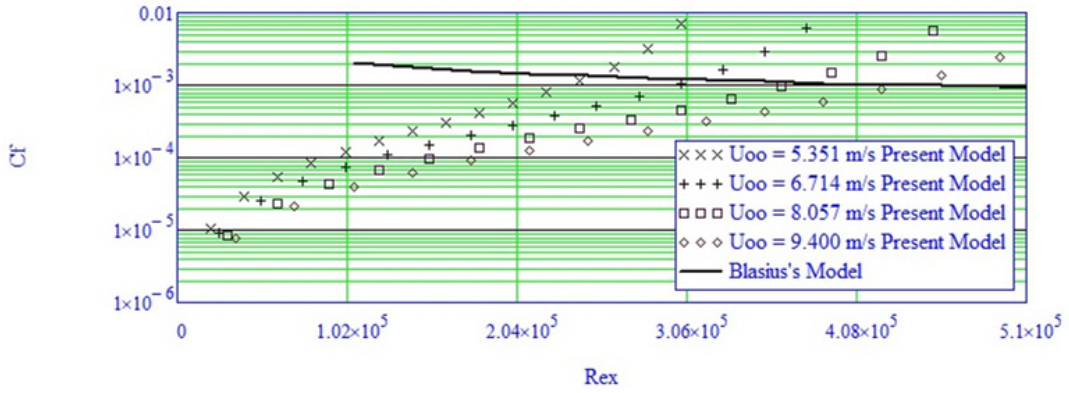


**Figure 8:** Local skin friction coefficient calculated by the present model, Equation (62), and by Blasius's [5] model, Equation (63), considering four stream velocity values.

## The classical relation between fluid friction and heat transfer

Equation (63) is a key component in demonstrating the Reynolds Analogy, while Equation (62) serves as the new expression replacing Equation (63). To establish the validity of the classic Reynolds Analogy for the flat plate, it is necessary to satisfy the conditions $\frac{1}{\beta(x)}=0.323$ and $p(XU_\infty)=\frac{1}{2}$ for a specific value of $Re_x$. However, in analyzing the behavior of factor $p(x,U_\infty)$, it is easy to see that there is no possibility of matching the requested conditions, even for a single situation, what compromises the Reynolds Analogy deduction departing from the flat plate correlations.

An alternative way to demonstrate the classical flat plate Reynolds Analogy is nevertheless possible because for turbulent flow over a flat plate or in a pipe, the exchange of mass, heat, and momentum occurs, mainly, by turbulence eddies. When these exchanges happen close to the wall, the main agent turns to be the molecular diffusion across the boundary layers, chiefly when the Prandtl or the Schmidt number is close to 1. Bennett & Myers et al. [33], on page 354, point out that the classical correlation

$$h=\frac{fU_\infty \rho cp}{2} \quad (64)$$

comes out from a proportionality based on intuition. Winterton [34] considers a correlation for the friction factor in a circular tube, valid for turbulent flow over smooth surfaces when the Reynolds number is greater than or about 4000, that is

$$f=0.046\,\mathrm{Re}^{-0.2} \quad (65)$$

According to Winterton [34], Equation (65) is only valid for channel flows but provides reasonable results for other geometries by evaluating the Reynolds number in terms of the equivalent diameter. Winterton [34] notes that for fully developed turbulent flow of a gas or non-metallic liquid in a smooth tube, the expression used to calculate the Nusselt number is that of Dittus and Boelter.

$$Nu=0.023Re^{0.8}Pr^{n} \quad (66)$$

where n=0.4 for heating, and n=0.3 for cooling. Consequently, for Pr=1, and considering Equations (65) to (66) we have:

$$St=\frac{f}{2} \quad (67)$$

Equation (67) indicates, in a simple way, the Reynolds analogy between heat and momentum transfer, showing that in turbulence, the same mechanism contributes to the transport of both heat and momentum. In fact, Sforza [35] reiterates that "The practical value of the Stanton number in heat transfer calculations arises from the Reynolds analogy between heat transfer and skin friction, which suggests that one is proportional to the other.".

## Conclusion

A rigorous mathematical treatment of Blasius's physical model of the flat plate boundary layer disregards the first non-null term of the serials solution as constant, and excludes the technique of finding out the root in the asymptotic zone of the non-dimensional x-direction velocity distribution. These procedures have completely changed the way of formulating Blasius equation and its solution, resulting in:

a. An equation able to overcome all the discussed incompatibilities present in the original equation and solution;

b. A model sensitive to possible combinations of circumstances associated with the position along the plate or influenced by the angle α(x), allowing the natural definition of the flow regime. This particularity represents a radical change in the conception of a different model as compared to orthodox ones. Traditional procedures require actions or elements to induce the laminar/turbulent transition, whatever the approach, theoretical, or experimental. For instance, the solution of the Orr-Sommerfeld equation, a crucial aspect of the incompressible stability theory, corresponds to small disturbance waves (Tollmien-Schlichting waves), Tuncer, and Cousteix [36]. These waves are also predicted by the simplified $e^n$-method, a significant tool in the field, as demonstrated by Roberts et al. [37]. On the other hand, experimental transition studies necessitate adjustments and the addition of components (such as tripping devices), leading to a non-spontaneous transition with potentially adverse effects. Schubauer and Skramstad [38], for example, discovered oscillations in the laminar boundary layer during a turbulent flat plate experiment by reducing the wind stream to low values using damping screens. Another example is the investigation by Schubauer & Klebanoff et al. [39] into how the transition occurs in a flat plate boundary layer,

using the technique proposed by Emmons [40] of intercepting the main flow with fences (spots).

c. The Reynolds flat plate analogy does not depend on the existence of similar equations, as previously conceived.

Figure 8 shows theoretical data corresponding to the behavior of an ongoing flow transition in the function of the variation of the local skin friction and the local Reynolds number. There is a comprehensive correspondence between the results calculated by Equations (62) of the present model and (63) due to Blasius [5], both concerned with the local skin coefficients. However, given its limitations, unlike the present model, Blasius´s model does not react to any "critical" flow conditions.

The velocity distributions in both x- and y-directions and the results of the boundary layer thickness stand for rational, theoretical, and practical comparisons.

## Data Availability

All data supporting the discussions and conclusions of this paper are found in the References.

## References


1. Jaguaribe EF (2020) Conflicting aspects in the flat plate boundary layer conventional solution. Math Probl Eng 2020: 1-8.
2. Jaguaribe EF (2021) Conflicting aspects in the flat plate boundary layer conventional solution. In: Shaikhet L (Eds.), Prime Archives in Applied Mathematics. (2nd edn), Vide Leaf, pp. 1-22.
3. Majdalani J, Xuan L (2020) On the Kármán momentum-integral approach and the Pohlhausen paradox. Physics of Fluids 32(12): 123605.
4. Prandtl L (1935) The mechanics of viscous fluids. Aerodynamic Theory 3: 208.
5. Blasius H (1907) Grenzschichten in flüssigkeiten mit kleiner reibung. Druck von BG Teubner.
6. Kármán TV (1921) Über laminare und turbulente Reibung. ZAMM-Journal of Applied Mathematics and Mechanics/Zeitschrift für Angewandte Mathematik und Mechanik 1(4): 233-252.
7. Karman TV (1946) On laminar and turbulent friction.
8. Pohlhausen K (1921) Zur näherungsweisen integration der differentialgleichung der laminaren grenzschicht. ZAMM-Journal of Applied Mathematics and Mechanics/Zeitschrift für Angewandte Mathematik und Mechanik 1(4): 252-290.
9. Pohlhausen K (1965) The approximate integration of the differential equation for the laminar boundary layer. Department of Aerospace Engineering, University of Florida, USA.
10. Tertevin N (1947) A review of boundary-layer literature.
11. Rohsenow WM, Choi H (1961) Heat, mass, and momentum transfer.
12. Pritchard PJ, John WM (2016) Fox and McDonald's introduction to fluid mechanics. John Wiley & Sons, USA.
13. Welty J, Gregory LR, David GF (2020) Fundamentals of momentum, heat and mass transfer. John Wiley & Sons, USA.
14. Nellis G, Sanford K (2008) Heat transfer. Cambridge university press, UK.
15. Howarth L (1938) On the solution of the laminar boundary layer equations. Proc Roy Soc 164(919).
16. Sissom LE, Donald R (1972) Elements of transport phenomena.
17. Töpfer C (1912) Bomerkungen zu dem aufsatz von h. Blasius, "grenzschichten in flüssigkeiten mit kleiner reibung," Z Math u Phys 60: 397-398.
18. Dyke VM (1975) Perturbation methods in fluid mechanics/annotated edition. Parabolic Press, California, USA, p. 284.
19. Na TY (1967) Transforming boundary conditions to initial conditions for ordinary differential equations. SIAM Review 9(2): 204-210.
20. Klamkin MS (1970) Transformation of boundary value problems into initial value problems. Journal of Mathematical Analysis and Applications 32(2): 308-330.
21. Zeldovich IB, Myshkis AD (1976) Elements of applied mathematics. MIR, Moscow, Russia.
22. Nickel K (1973) Prandtl's boundary-layer theory from the viewpoint of a mathematician. Annual Review of Fluid Mechanics 5(1): 405-428.
23. Joslin RD, Criminale WO, Jackson TL (2010) Theory and computation of hydrodynamic stability. Cambridge University Press, UK.
24. Parveen S (2016) Numerical solution of non-linear differential equation by using shooting techniques. International Journal of Mathematics and Its Applications 4(1-A): 93-100.
25. Jaguaribe EF (2022) The flat plate boundary layer equation under Blasius restrictions with a unique solution. Math Probl Eng 2022: 1-9.
26. Hermann S, Kestin J, Street R (1980) Boundary-layer theory. pp. 125-125.
27. Benjamin Fine and Gerhard Rosenberger (1997) The fundamental theorem of algebra. Springer, New York, pp. 1-210.
28. Meserve, Bruce Elwyn (1982) Fundamental concepts of algebra. Dover Publications, New York, pp. 281-283.
29. Bhoraniya R, Gayathri S, and Vinod N (2003) Global stability analysis of shear flows. Springer, Germany.
30. Morkovin MV, Reshotko E (1979) Dialogue on progress and issues in stability and transition research. Laminar-Turbulent Transition: IUTAM-International Union of Theoretical and Applied Mechanics, pp. 3-29.
31. Puttkammer PP (2013) Boundary layer over a flat plate. University of Twente, Netherlands.
32. Clayton TC, Donald FE, John AR (2002) Engineering fluid mechanics. pp. 15-60.
33. Bennett, Carroll O, John Earle M (1982) Momentum, heat, and mass transfer.
34. Winterton, Richard HS (2014) Thermal design of nuclear reactors. Elsevier, Netherlands.
35. Sforza PM (2015) Manned spacecraft design principles. Elsevier, Netherlands.
36. Cousteix J, Cebeci T (20225) Modeling and computation of boundary-layer flows: laminar, turbulent and transitional boundary layers in incompressible and compressible flows. Berlin, Springer, Germany.
37. Roberts L, Correia J, Finnis M, Knowles k (2014) Investigation of forcing boundary layer transition on a single-element inverted wing in ground effect. International Vehicle Aerodynamics Conference, pp. 199-211.
38. Schubauer GB, Skramstad HK (1947) Laminar boundary-layer oscillations and transition on a flat plate. Journal of research of the National Bureau of Standards 38: 251-292.
39. Schubauer GB, Klebanoff PS (1955) Contributions on the mechanics of boundary-layer transition. NACA-TR, USA, pp. 853-863.
40. Emmons HW (1951) The laminar-turbulent transition in a boundary layer-Part I. Journal of the Aeronautical Sciences 18(7): 490-498.